First Constraints on the Complete Neutrino Mixing Matrix with a Sterile Neutrino

G. H. Collin, C. A. Argüelles, J. M. Conrad, and M. H. Shaevitz

Phys. Rev. Lett. **117**, 221801 — Published 23 November 2016

DOI: 10.1103/PhysRevLett.117.221801

First Constraints on the Complete Neutrino Mixing Matrix with a Sterile Neutrino

G.H. Collin[1], C.A. Argüelles[1], J.M. Conrad[1], M.H. Shaevitz[2]
[1] *Massachusetts Institute of Technology, Cambridge, MA 02139, USA and*
[2] *Columbia University, New York, NY 10027, USA*

Neutrino oscillation models involving one extra mass eigenstate beyond the standard three (3+1) are fit to global short baseline experimental data and the recent IceCube $\nu_\mu + \bar{\nu}_\mu$ disappearance search result. We find a best fit of $\Delta m^2_{41} = 1.75$ eV^2 with $\Delta\chi^2_{null-min}$/dof of 50.61/4. We find that the combined IceCube and short baseline data constrain θ_{34} to $< 80°(< 6°)$ at 90% C.L. for $\Delta m^2_{41} \approx 2(6)$ eV^2, which is improved over present limits. Incorporating the IceCube information provides the first constraints on all entries of the 3+1 mixing matrix.

PACS numbers: 14.60.Pq,14.60.St

INTRODUCTION

The quantum-mechanical effect of neutrino oscillations, observed in multiple experiments [1], occurs if the neutrino mass eigenstates are mixtures of flavor eigenstates. Most neutrino oscillation data sets fit well into a model involving three active neutrinos that map to three distinct mass states through a unitary mixing matrix [1]. This model has two independent squared-mass splittings, $\Delta m^2_{ji} = m^2_j - m^2_i$ which set the frequency of the oscillations. The larger of the two splittings, historically called the atmospheric splitting, is $\Delta m^2_{atm} = 2.3 \times 10^{-3}$eV^2 [2], while the smaller well-confirmed splitting, called the solar splitting, is $\Delta m^2_{sol} = 7.5 \times 10^{-5}$eV^2 [2].

However, a set of experiments [3–9] report anomalous results consistent with a substantially different frequency than the solar and atmospheric oscillations. These experiments, classified as "short baseline" (SBL), are designed with a travel-distance-to-energy ratio for the neutrino of around $L/E \sim 1$m/MeV. The significance of these signals ranges from 2σ to 4σ, and hence each are less compelling, individually, than the solar and atmospheric results. However, taken together, the results point to a new oscillation parameter region with a splitting of $\Delta m^2 \sim 1$ eV^2. To accommodate this, one can introduce a fourth neutrino mass and flavor state. Since LEP Z^0 decay measurements are consistent with only three low mass, active neutrinos [10], an additional fourth neutrino flavor must be inactive, historically called "sterile." With this said, other SBL experiments sensitive to this oscillation frequency have observed null results [11–20]. These limits must be accounted for in any model with extra neutrino flavors. As a result, global fits to the data of models with three active and one sterile neutrino ("3+1" models) have a limited allowed range in vacuum oscillation parameter space [21–23]. A suite of new SBL experiments, which are now underway [24] or are in design [25–28] have been prompted by these global fits.

In Ref. [21], we reported the results of global fits to the SBL data that yielded 90% CL allowed regions at three Δm^2 values of, approximately, 1, 1.75 and 6 eV^2. In this paper, we expand these 3+1 fits to include a new, highly restrictive oscillation limit from the IceCube Experiment [29] that reduces the allowed parameter space. Because the IceCube analysis relies on matter effects rather than vacuum oscillations, this new data set breaks degeneracies, allowing, for the first time, to fill in all of the elements of the 3+1 mixing matrix.

CONSTRAINTS FROM SBL EXPERIMENTS

SBL experiments have direct sensitivity to neutrino oscillations involving electron and muon flavor neutrinos, but do not have direct sensitivity to transitions involving the tau neutrino flavor. This is because the ν_τ threshold for charged current (CC) interactions of 3.4 GeV suppresses CC interactions for these low energy SBL experiments. A full 3+1 model, however, has a 4×4 matrix that connects all three active plus single sterile flavor states to the four mass states:

$$U_{3+1} = \begin{bmatrix} U_{e1} & U_{e2} & U_{e3} & U_{e4} \\ U_{\mu 1} & U_{\mu 2} & U_{\mu 3} & U_{\mu 4} \\ U_{\tau 1} & U_{\tau 2} & U_{\tau 3} & U_{\tau 4} \\ U_{s1} & U_{s2} & U_{s3} & U_{s4} \end{bmatrix}. \quad (1)$$

The SBL experiments can only directly constrain the elements U_{e4} and $U_{\mu 4}$.

Because the observed anomalous mass splitting of 1 eV^2 is large compared to the solar and atmospheric cases, one can make the approximations that $\Delta m^2_{41} \approx \Delta m^2_{42} \approx \Delta m^2_{43}$ and $\Delta m^2_{21} \approx \Delta m^2_{32} \approx 0$. This leads to the SBL approximation for the vacuum oscillation probability formula for $\nu_\alpha \to \nu_\beta$:

$$P_{\alpha\beta} = \delta_{\alpha\beta} - 4(\delta_{\alpha\beta} - U_{\alpha 4}U^*_{\beta 4})U^*_{\alpha 4}U_{\beta 4}\sin^2\left(\frac{\Delta m^2_{41}L}{4E}\right). \quad (2)$$

In this equation, L is the distance the neutrino travels and E is the energy of the neutrino. For flavors α and β, this is equivalent to a two neutrino model with a mixing amplitude of

$$\sin^2 2\theta_{\alpha\beta} = |4(\delta_{\alpha\beta} - U_{\alpha 4}U^*_{\beta 4})U^*_{\alpha 4}U_{\beta 4}|. \quad (3)$$

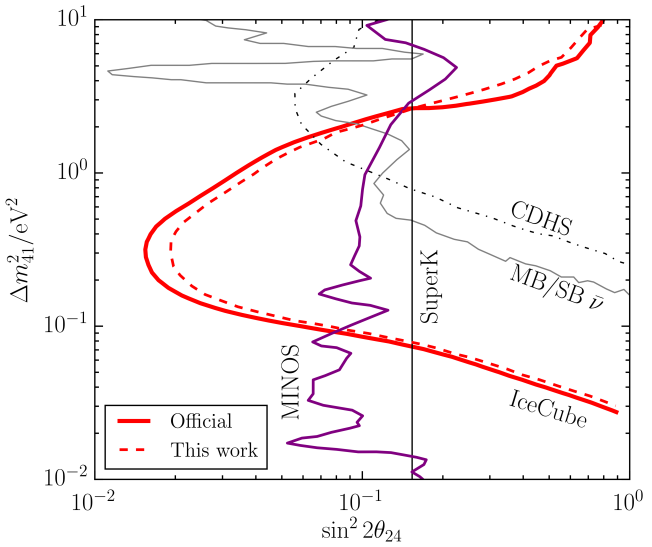

FIG. 1: Comparison of 90% CL limits for muon flavor disappearance of IceCube 2016, MINOS 2016, CDHS and MiniBooNE-SciBooNE. Our reconstruction of the IceCube result using the data release is indicated by the dashed line.

Thus, in this notation, muon-to-electron flavor appearance experiments measure $\sin^2 2\theta_{\mu e}$, and the disappearance experiments measure $\sin^2 2\theta_{ee}$ and $\sin^2 2\theta_{\mu\mu}$.

The SBL experiments used in the fit are chosen to be relevant in the range of $\Delta m^2 > 0.3$ eV^2 at 90% CL, which is the limit of LSND [3]. We fit in the range of $0.1 < \Delta m^2 < 100$ eV^2. The specifics of the SBL data sets are given in Table 1 of Ref. [21], and the associated text, and so we very briefly explain the choices here. With respect to electron neutrino appearance, we include LSND [3], MiniBooNE (ν and $\bar{\nu}$ from the BNB flux) [4, 5, 30, 31], MiniBooNE (NuMI off-axis ν flux) [32], KARMEN [11] and NOMAD[16]. With respect to electron neutrino disappearance, we include Bugey [6], the Gallium Experiments [8, 9] and the Karmen/LSND cross section analysis [12]. With respect to ν_μ disappearance, we include the MiniBooNE-SciBooNE joint analyses in ν and $\bar{\nu}$ running [33, 34], the CDHS result [18], MINOS results from 2006 and 2008 [19, 35] that are strictly from CC analysis, and CCFR84 [17].

There are two results published in 2016 that are not included in these fits. The 2016 Daya Bay $\bar{\nu}_e$ disappearance result, which addresses $2 \times 10^{-4} < \Delta m^2 < 0.3$ eV^2 [36], need not be included in these fits. The small overlap is in a region dominated by the Bugey result [6]. The 2016 MINOS ν_μ disappearance result [37] is not included in the fit for two reasons. First, this result is not competitive with the IceCube and other data sets already used in the region of interest, as seen in Fig. 1. Second, this disappearance result incorporates neutral current data, with a background subtraction for the relatively large [38] ν_e intrinsic flux. Thus the MINOS limit is dependent on their assumption that $|U_{e4}|^2 = 0$ and cannot be directly used in global fits that need to include ν_e disappearance in an unrestricted way.

These fits also do not include data from cosmology because the CMB and large scale structure (LSS) constraints on the presence of a fourth neutrino are model dependent. The dependencies include assuming a "standard" thermal history for the Universe [39]. Sterile neutrino thermalization can be suppressed a number of plausible ways [40–48]. Thermalization may not occur when one considers models with full four-neutrino mixing [49]. Introducing the assumption that sterile neutrinos have very weak pseudoscalar interactions that are unobservable in the SBL data not only resolves the apparent disagreement between the 3+1 models and CMB, it also predicts a Hubble constant in agreement with local measurements [50]. Changes in the assumption of the influence of dark energy on the expansion history and growth structure also influences the comological results [39]. Based on this, it is most interesting is to fit the cosmological data separately from the oscillation experiments, and then consider the meaning of discrepancies.

The global fit favors a model with one mass state dominated by the sterile flavor. The three assumed degenerate mass states are dominated by the active flavors, as is demanded by the solar and atmospheric neutrino results. The SBL fits cannot distinguish the mass hierarchy, that is, whether the dominantly sterile flavor is the highest mass state, which is called a 3+1 hierarchy, or the lowest mass state, which is called a 1+3 hierarchy.

INCORPORATING ICECUBE DATA

We now expand the 3+1 fits to include data from IceCube [29], which is quite different in design from the SBL experiments. It makes use of measurements of the atmospheric ν_μ flux, as a function of the zenith angle and energy in the range from 400 GeV to 20 TeV. The detector consists of 86 strings of optical modules located within the Antarctic ice. The energy and path-length through the Earth is equivalent to an $L/E \sim 1$ m/MeV value, similar to the SBL experiments. However, the strength of the IceCube null result, shown in Fig. 1, arises from the additional modifications of the oscillation behavior when high energy neutrinos travel through dense matter, called "matter effects."

The matter-effect signature in IceCube corresponds to a predicted large deficit in the antineutrino flux for the up-going neutrinos that cross the Earth, given a 3+1 model with an anomalous squared mass splitting of ~ 1 eV^2 [51–57]. This modification to the vacuum oscillation formalism comes from differences between neutrino charged- and neutral-current interactions with the earth. In experiments at low energy or short baselines, this ef-

fect is negligible. However, at the high energies and long baselines available to the IceCube experiment, coherent forward scattering can significantly affect neutrino propagation. In a 3+1 model, an additional matter potential is introduced to account for the difference of active flavor neutrinos scattering from matter–a contribution that is missing for the sterile flavor.

The matter effect is dependent on the neutrino mass hierarchy. In the case of a $3+1$ hierarchy, as opposed to a $1+3$ hierarchy, the matter-induced resonance will appear in the antineutrino events rather than the neutrino events. Detectable effects will lie in the range $0.01 \leq \Delta m^2 \leq 10$ eV^2—the region of interest for our global fits. This follows from the the resonant energy: $E_{res} = \frac{\cos 2\theta \Delta m^2}{\sqrt{2} G_F N_{nuc}}$, where θ is an effective two flavor active-to-sterile neutrino mixing angle and N_{nuc} is the target number density. The quoted sensitivity range can be understood by replacing N_{nuc} by the corresponding density of the Earth, and the energy by the energy thresholds of the data set. It should be noted that the IceCube null result leads to a more restrictive limit in the case of 1+3 compared to a 3+1 model. This comes about because about 70% of the events in IceCube are due to neutrino interactions, where a 1+3 signal would appear. This is in agreement with the conclusions of cosmology and further justifies our concentration on 3+1 models below.

Use of matter effects in the IceCube analysis breaks degeneracies in the fits, allowing, for the first time, to constrain all of the elements of the 3+1 mixing matrix. Examining Eq. 1, one sees that the matrix has elements determined by the atmospheric and solar oscillation measurements, for which we use the results of Ref. [58] as the range of allowed values. This leaves seven further elements. Four of these elements, $(U_{s1}, \ldots, U_{s4})$, cannot be directly constrained by experiment due to the non-interacting nature of the 'sterile' flavor state. However, in a 3+1 model, the mixing matrix is unitary, and so these unmeasureable elements can be determined if the remaining three matrix elements are constrained. This leaves the elements U_{e4}, $U_{\mu 4}$ and $U_{\tau 4}$ to be determined from the global fits to the combined SBL and IceCube data sets that we present below.

The SBL approximation, which has been applied in our previous fits [21], cannot be applied when including the matter-effect signature in IceCube. In our global analysis, the νSM values of 7.5×10^{-5}eV^2 and 2.3×10^{-3}eV^2 from Ref. [2] are used for Δm^2_{sol} and Δm^2_{atm}, respectively. Furthermore, the introduction of IceCube data requires a parameterization of the extended lepton mixing matrix, Eq. 1. This can be presented as a product of rotations following the convention specified in Ref. [59]:

$$U_{3+1} = R_{34} R_{24} R_{14} R_{23} R_{13} R_{12}. \quad (4)$$

Each R_{ij} is a rotation matrix through angle θ_{ij} in the ij plane. In this parameterization, the fourth column of

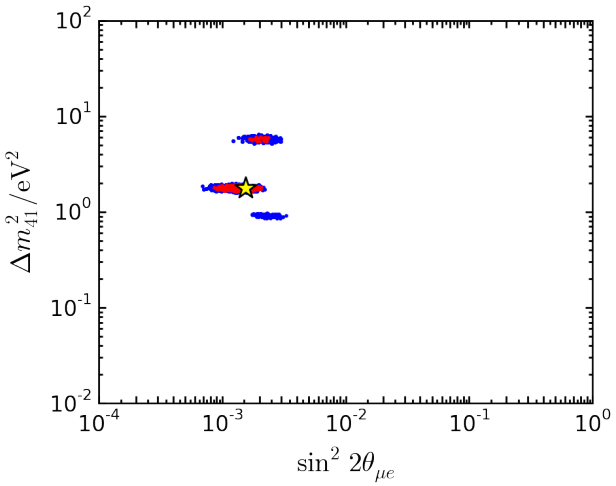

FIG. 2: Frequentist $3+1$ global fit for SBL+IceCube: Δm^2_{41} vs $\sin^2 2\theta_{\mu e}$. Red – 90% CL; Blue –99% CL.

U_{3+1} is given by

$$u_4 = (\sin\theta_{14}, \cos\theta_{14}\sin\theta_{24}, \cos\theta_{14}\cos\theta_{24}\sin\theta_{34}, \cos\theta_{14}\cos\theta_{24}\cos\theta_{34})^T . \quad (5)$$

If one sets all the CP violating phases to zero, only three new angles are introduced: θ_{14}, θ_{24}, and θ_{34}. In addition, the IceCube collaboration analysis assumes $\theta_{14} = \theta_{34} = 0$. Under these assumptions, $\sin^2 2\theta_{24} = \sin^2 2\theta_{\mu\mu}$—the vacuum disappearance amplitude. While this is a convenient way to express the ν_μ disappearance result (and is used in Ref. [29] along with other papers), these assumptions will need to be relaxed in order to include IceCube in the global fits.

The IceCube analysis and the results presented here make use of nuSQuIDS software [59, 60] that models flavor evolution from three (*i.e.* νSM) to six flavor basis states with customized matter potentials. The 3+1 nuSQuIDS calculation does not use the SBL approximation; thus, it includes the two additional CP violating parameters that arise when Δm^2_{21} and Δm^2_{31} are nonzero and unequal. However, in the case of the IceCube analysis, these CP parameters are set to zero. For the matter potential, nuSQuIDS makes use of the Preliminary Reference Earth Model (PREM) [61] parameterization describing the radial density profile of the Earth. The neutrino propagation implementation follows Eqs. (29-30) in Ref. [62]. For the neutrino nucleon cross sections, we use the perturbative QCD calculation from Ref. [63, 64].

No evidence for anomalous ν_μ or $\overline{\nu}_\mu$ disappearance was observed in the IceCube data set. The resulting stringent limit extends to $\sin^2 2\theta_{24} \leq 0.02$ at $\Delta m^2 \sim 0.3$ eV^2 at 90% CL for $\theta_{34} = 0$ [29]. To incorporate this result into the fit, we must relate the mixing angles θ_{14}, θ_{24}, and θ_{34} to the short-baseline neutrino oscillation probabilities. The oscillation amplitudes in this parameterization are found

3+1	Δm^2_{41}	$\lvert U_{e4}\rvert$	$\lvert U_{\mu 4}\rvert$	$\lvert U_{\tau 4}\rvert$	N_{bins}	$\chi^2_{\rm min}$	$\chi^2_{\rm null}$	$\Delta\chi^2$ (dof)
SBL	1.75	0.163	0.117	-	315	306.81	359.15	52.34 (3)
SBL+IC	1.75	0.164	0.119	0.00	524	518.23	568.84	50.61 (4)
IC	5.62	-	0.314	-	209	207.11	209.69	2.58 (2)

TABLE I: The oscillation parameter best-fit points for $3+1$ for the combined SBL and IceCube data sets compared to SBL alone. Units of Δm^2 are eV^2.

Δm^2/eV^2	$\lvert U_{e4}\rvert$	$\lvert U_{\mu 4}\rvert$	$\lvert U_{\tau 4}\rvert$	θ_{34}
6	[0.17,0.21]	[0.10,0.13]	[0.00,0.05]	$< 6^\circ$
2	[0.13,0.20]	[0.09,0.15]	[0.00,0.70]	$< 80^\circ$

TABLE II: The 90% CL regions for matrix elements and the upper limit on θ_{34} for the two allowed regions in Δm^2. For $\Delta m^2 = 1$ eV^2 there are no allowed regions at 90%CL

by substituting the matrix elements in Eq. (5) into Eq. (2); e.g., $\sin^2 2\theta_{\mu e} = \sin^2 2\theta_{14} \sin^2 \theta_{24}$. Since the short baseline anomalies imply $\sin^2 2\theta_{\mu e} \neq 0$, it follows that we cannot assume $\theta_{14} = 0$ in a global fit.

It has been shown [65] that the presence of the matter-induced resonance critically depends on the value of θ_{34}. When θ_{34} is maximal, there is no matter-induced resonant enhancement. On the other hand, as noted by Ref. [54], increasing θ_{34} distorts the atmospheric $\nu_\mu \to \nu_\tau$ neutrino oscillation. The interplay between these effects makes the IceCube data sensitive to θ_{34}. We obtain the constraint on this parameter by sampling logarithmically in $\sin^2(2\theta_{34})$ from 10^{-3} to 1. The CP phases have a subleading contribution in comparison to the θ_{34} effect [54]; thus, they have been set to zero.

We describe the techniques of including the IceCube data into the fits in the appendix to this article. Our reproduction of the IceCube result using the data release is shown in Fig. 1, dashed. The IceCube likelihood must be converted to a χ^2 that can be combined with the SBL data. The high computational cost of propagating neutrino fluxes through the Earth with nuSQuIDS prevents the analysis from being directly included into the global fitting software. Instead, the global fits were used to find a reduced set of parameters ("test points") that could be evaluated directly. This assumes that the effect of IceCube on the global fit is a small perturbation, which is reasonable given that the IceCube-only $\Delta\chi^2$ is small compared to the SBL only global fit $\Delta\chi^2$ (see Table I).

RESULTS

Figs. 2 and 3 show the SBL+IceCube global $3+1$ fit result. The former shows Δm^2_{41} vs $\sin^2 2\theta_{\mu e}$, as defined in Eq. 3. The latter presents the result as a function of the mixing matrix elements. The $\lvert U_{\tau 4}\rvert$ result is presented on a linear scale because one test point, the preferred solution, is $\lvert U_{\tau 4}\rvert = 0$.

The IceCube data exclude the solution at ~ 1 eV^2 at 90% CL, although that solution persists at 99% CL. This has important implications for future sterile neutrino searches designed to address the 1 eV^2 allowed region. For example, given the peak energy of the BNB neutrino beam [25], the position of the ICARUS T600 detector at Fermilab will result in a large potential signal for 1 eV^2 sterile neutrino, but less so if the Δm^2 is higher.

As discussed, the SBL experiments constrain $\lvert U_{e4}\rvert$ and $\lvert U_{\mu 4}\rvert$, while the IceCube analysis has strong dependence on $\lvert U_{\mu 4}\rvert$ and $\lvert U_{\tau 4}\rvert$ through the matter-induced resonance. Thus, including IceCube provides insight into the less explored $\lvert U_{\tau 4}\rvert$ parameter. Using $\lvert U_{\tau 4}\rvert = \cos\theta_{14}\cos\theta_{24}\sin\theta_{34}$, we convert the results to the 90% C.L. ranges in Tab. II. At $\Delta m^2 \sim 6$ eV^2, our limit improves the bound of $\theta_{34} < 25^\circ$ at 90% C.L. from MINOS [66] by a factor of four.

This new result on $\lvert U_{\tau 4}\rvert$ allows us to have a first complete picture of the extended lepton mixing matrix:

$$|U| = \begin{bmatrix} 0.79 \to 0.83 & 0.53 \to 0.57 & 0.14 \to 0.15 & 0.13\ (0.17) \to 0.20\ (0.21) \\ 0.25 \to 0.50 & 0.46 \to 0.66 & 0.64 \to 0.77 & 0.09\ (0.10) \to 0.15\ (0.13) \\ 0.26 \to 0.54 & 0.48 \to 0.69 & 0.56 \to 0.75 & 0.0\ (0.0) \to 0.7\ (0.05) \\ \cdots & \cdots & \cdots & \cdots \end{bmatrix}. \quad (6)$$

Above, "..." represents parameters constrained by the unitarity of the 4×4 matrix. The ranges in the matrix correspond to 90% confidence intervals. The entries in the last column correspond to this work and are given for $\Delta m^2 \sim 2$ eV^2 ($\Delta m^2 \sim 6$ eV^2). The intervals shown in each entry for the standard 3×3 submatrix were obtained from Ref. [67], and are independent of our fit. As a check of consistency, our values in the fourth column can be compared with the upper bounds from the 3×3 non-unitarity analysis in Ref. [67], which gave $\lvert U_{e4}\rvert < 0.27$, $\lvert U_{\mu 4}\rvert < 0.73$, and $\lvert U_{\tau 4}\rvert < 0.623$ at 90% CL. Our results in Eq. 6 are fully compatible with these upper limits, which are based on standard 3-neutrino oscillation measurements exclusive of any sterile neutrino search data.

CONCLUSION

We have presented three new results. First, we have presented a combined fit of SBL and IceCube data result-

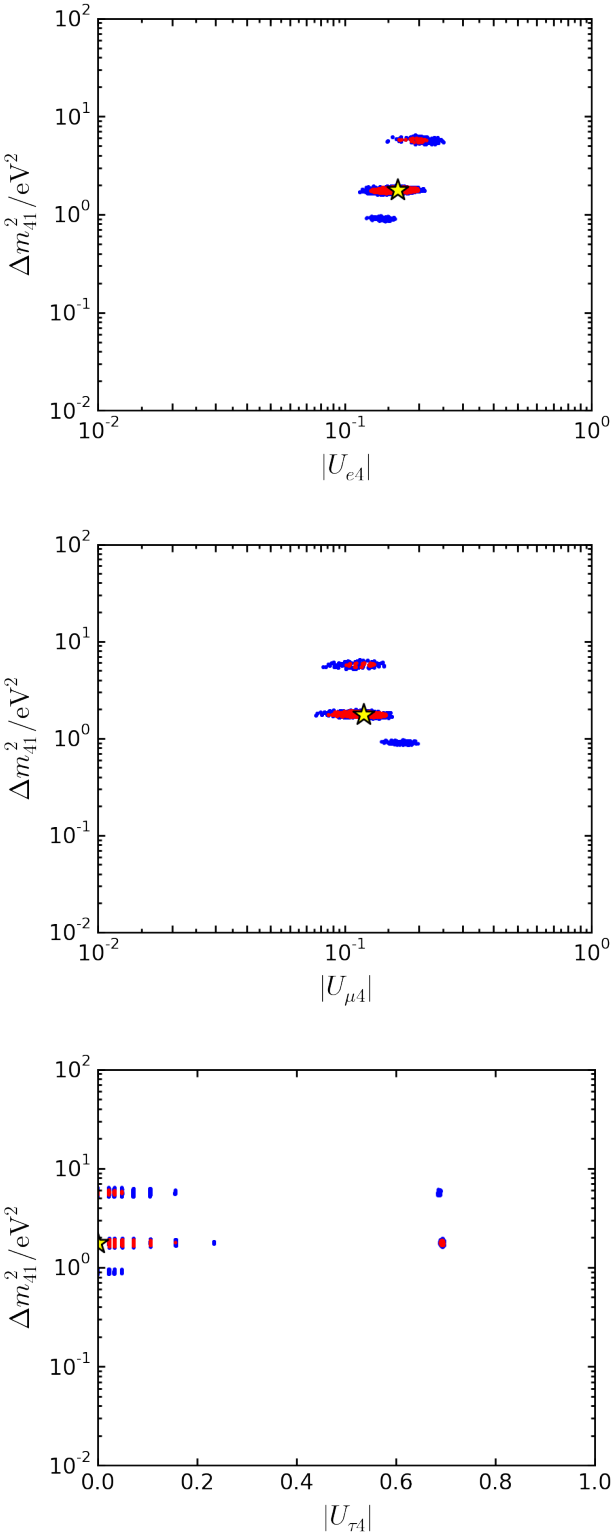

FIG. 3: Frequentist 3 + 1 global fit SBL+IceCube, shown as a function of matrix element: $|U_{e4}|$ (top), $|U_{\mu 4}|$ (middle), and $|U_{\tau 4}|$ (bottom). Red – 90% CL; blue–99% CL.

ing in a best fit of $\Delta m^2_{41} = 1.75$ eV^2 with $\Delta\chi^2_{null-min}$ of 50.61 for 4 dof. The IceCube data substantially lessens the likelihood of the ~ 1 eV^2 allowed region that was, until recently, the best fit point [68]. Second, we have shown that this fit is sensitive to $|U_{\tau 4}|$, providing improved constraint on θ_{34} of $< 80°(< 6°)$ at 90% C.L. for $\Delta m^2_{41} \approx 2(6)$ eV^2. Lastly, we have used this, along with constraints from fits to atmospheric and solar data sets, to fill in all components of the 3+1 mixing matrix for the first time.

Acknowledgements

GC, CA and JC are supported by NSF grants 1505858 and 1505855, and MS is supported by NSF grant 1404209. We thank Kevork Abazajian, Christina Ignarra, Benjamin Jones, William Louis, and Jordi Salvado for useful discussion. We thank Maxim Goncharov for computing support.

[1] K. A. Olive et al. (Particle Data Group), Chin. Phys. **C38**, 090001 (2014).

[2] M. Gonzalez-Garcia, M. Maltoni, and T. Schwetz, Journal of High Energy Physics **2014**, 52 (2014), URL http://dx.doi.org/10.1007/JHEP11%282014%29052.

[3] A. Aguilar-Arevalo et al. (LSND Collaboration), Phys. Rev. D **64**, 112007 (2001).

[4] A. A. Aguilar-Arevalo et al. (MiniBooNE), Phys. Rev. Lett. **110**, 161801 (2013), 1207.4809.

[5] A. A. Aguilar-Arevalo et al. (MiniBooNE), Phys. Rev. Lett. **102**, 101802 (2009), 0812.2243.

[6] Y. Declais, J. Favier, A. Metref, H. Pessard, B. Achkar, et al., Nucl. Phys. B **434**, 503 (1995).

[7] G. Mention, M. Fechner, T. Lasserre, T. A. Mueller, D. Lhuillier, M. Cribier, and A. Letourneau, Phys. Rev. **D83**, 073006 (2011), 1101.2755.

[8] J. Abdurashitov et al. (SAGE Collaboration), Phys. Rev. C **80**, 015807 (2009).

[9] F. Kaether, W. Hampel, G. Heusser, J. Kiko, and T. Kirsten, Phys. Lett. B **685**, 47 (2010).

[10] ALEPH Collaboration, DELPHI Collaboration, L3 Collaboration, OPAL Collaboration, SLD Collaboration, LEP Electroweak Working Group, SLD Electroweak and Heavy Flavour Groups, Phys. Rept. **427**, 257 (2006).

[11] B. Armbruster et al. (KARMEN Collaboration), Phys. Rev. D **65**, 112001 (2002).

[12] J. Conrad and M. Shaevitz, Phys. Rev. D **85**, 013017 (2012).

[13] P. Adamson et al. (MiniBooNE and MINOS Collaborations), Phys. Rev. Lett. **102**, 211801 (2009).

[14] A. A. Aguilar-Arevalo et al. (MiniBooNE Collaboration), Phys. Rev. Lett. **103**, 061802 (2009).

[15] G. Cheng et al. (SciBooNE Collaboration), Phys. Rev. D **84**, 012009 (2011).

[16] P. Astier et al. (NOMAD Collaboration), Phys. Lett. B **570**, 19 (2003).

[17] I. Stockdale, A. Bodek, F. Borcherding, N. Giokaris, K. Lang, et al., Z. Phys. C **27**, 53 (1985).

[18] F. Dydak, G. Feldman, C. Guyot, J. Merlo, H. Meyer, et al., Phys. Lett. B **134**, 281 (1984).

[19] D.G. Michael *et al.* (MINOS Collaboration), Phys. Rev. Lett. **97**, 191801 (2006).

[20] P. Adamson *et al.* (MINOS Collaboration), Phys. Rev. Lett. **101**, 131802 (2008).

[21] G. H. Collin, C. A. Argelles, J. M. Conrad, and M. H. Shaevitz, Nucl. Phys. **B908**, 354 (2016), 1602.00671.

[22] J. Kopp, P. A. N. Machado, M. Maltoni, and T. Schwetz, Journal of High Energy Physics **2013** (2013), ISSN 1029-8479, arXiv: 1303.3011, URL http://arxiv.org/abs/1303.3011.

[23] C. Giunti, M. Laveder, Y. F. Li, and H. W. Long, Physical Review D **88** (2013), ISSN 1550-7998, 1550-2368, arXiv: 1308.5288, URL http://arxiv.org/abs/1308.5288.

[24] H. Chen *et al.* (MicroBooNE Collaboration) (2007), "Proposal for a New Experiment Using the Booster and NuMI Neutrino Beamlines: MicroBooNE", URL http://www-microboone.fnal.gov/public/MicroBooNE_10152007.pdf.

[25] M. Antonello et al. (LAr1-ND, ICARUS-WA104, MicroBooNE) (2015), 1503.01520.

[26] A. Adelmann, J. Alonso, W. A. Barletta, J. M. Conrad, M. H. Shaevitz, J. Spitz, M. Toups, and L. A. Winslow, Adv. High Energy Phys. **2014**, 347097 (2014), 1307.6465.

[27] T. J. Langford (PROSPECT), Nucl. Part. Phys. Proc. **265-266**, 123 (2015), 1501.00194.

[28] D. Bravo-Berguo et al. (SOX), Nucl. Part. Phys. Proc. **273-275**, 1760 (2016).

[29] M. G. Aartsen et al. (IceCube) (2016), 1605.01990.

[30] A. A. Aguilar-Arevalo et al. (MiniBooNE), Phys. Rev. Lett. **98**, 231801 (2007), 0704.1500.

[31] A. A. Aguilar-Arevalo et al. (MiniBooNE), Phys. Rev. Lett. **105**, 181801 (2010), 1007.1150.

[32] P. Adamson et al. (MiniBooNE, MINOS), Phys. Rev. Lett. **102**, 211801 (2009), 0809.2447.

[33] K. B. M. Mahn et al. (SciBooNE, MiniBooNE), Phys. Rev. **D85**, 032007 (2012), 1106.5685.

[34] G. Cheng et al. (SciBooNE, MiniBooNE), Phys. Rev. **D86**, 052009 (2012), 1208.0322.

[35] P. Adamson *et al.* (MINOS Collaboration), Phys. Rev. D **77**, 072002 (2008).

[36] F. P. An et al. (Daya Bay) (2016), 1607.01174.

[37] P. Adamson et al. (MINOS), Submitted to: Phys. Rev. Lett. (2016), 1607.01176.

[38] P. Adamson et al. (MINOS), Phys. Rev. Lett. **107**, 181802 (2011), 1108.0015.

[39] K. N. Abazajian and M. Kaplinghat, Ann Rev. Nuc. Part. Phys. **66**, 401 (2016).

[40] K. N. Abazajian, Astropart. Phys. **19**, 303 (2003), astro-ph/0205238.

[41] B. Dasgupta and J. Kopp, Phys. Rev. Lett. **112**, 031803 (2014), 1310.6337.

[42] S. Hannestad, R. S. Hansen, and T. Tram, Phys. Rev. Lett. **112**, 031802 (2014), 1310.5926.

[43] L. Bento and Z. Berezhiani, Phys. Rev. **D64**, 115015 (2001), hep-ph/0108064.

[44] Y.-Z. Chu and M. Cirelli, Phys. Rev. **D74**, 085015 (2006), astro-ph/0608206.

[45] R. Foot and R. R. Volkas, Phys. Rev. Lett. **75**, 4350 (1995), hep-ph/9508275.

[46] G. Gelmini, S. Palomares-Ruiz, and S. Pascoli, Phys. Rev. Lett. **93**, 081302 (2004), astro-ph/0403323.

[47] C. M. Ho and R. J. Scherrer, Phys. Rev. **D87**, 065016 (2013), 1212.1689.

[48] J. Hamann, S. Hannestad, G. G. Raffelt, and Y. Y. Y. Wong, JCAP **1109**, 034 (2011), 1108.4136.

[49] K. Abazajian, N. F. Bell, G. M. Fuller, and Y. Y. Y. Wong, Phys. Rev. **D72**, 063004 (2005), astro-ph/0410175.

[50] M. Archidiacono, S. Gariazzo, C. Giunti, S. Hannestad, R. Hansen, M. Laveder, and T. Tram, JCAP **1608**, 067 (2016), 1606.07673.

[51] H. Nunokawa, O. L. G. Peres, and R. Zukanovich Funchal, Phys. Lett. **B562**, 279 (2003), hep-ph/0302039.

[52] S. Choubey, JHEP **12**, 014 (2007), 0709.1937.

[53] S. Razzaque and A. Yu. Smirnov, Phys. Rev. **D85**, 093010 (2012), 1203.5406.

[54] A. Esmaili and A. Yu. Smirnov, JHEP **12**, 014 (2013), 1307.6824.

[55] V. Barger, Y. Gao, and D. Marfatia, Phys. Rev. **D85**, 011302 (2012), 1109.5748.

[56] A. Esmaili, F. Halzen, and O. L. G. Peres, JCAP **1211**, 041 (2012), 1206.6903.

[57] A. Esmaili, F. Halzen, and O. L. G. Peres, JCAP **1307**, 048 (2013), 1303.3294.

[58] S. Parke and M. Ross-Lonergan (2015), 1508.05095.
[59] C. A. Arguelles Delgado, J. Salvado, and C. N. Weaver (2014), 1412.3832.
[60] C. A. Arguelles Delgado, J. Salvado, and C. N. Weaver, *ν-SQuIDS*, https://github.com/arguelles/nuSQuIDS.
[61] A. M. Dziewonski and D. L. Anderson, Physics of the Earth and Planetary Interiors **25**, 297 (1981).
[62] M. C. Gonzalez-Garcia, F. Halzen, and M. Maltoni, Phys. Rev. **D71**, 093010 (2005), hep-ph/0502223.
[63] C. A. Arguelles, F. Halzen, L. Wille, M. Kroll, and M. H. Reno, Phys. Rev. **D92**, 074040 (2015), 1504.06639.
[64] A. Cooper-Sarkar, P. Mertsch, and S. Sarkar, JHEP **08** (2011), 1106.3723, URL http://arxiv.org/abs/1106.3723.
[65] M. Lindner, W. Rodejohann, and X.-J. Xu (2015), 1510.00666.
[66] P. Adamson et al. (MINOS), Phys. Rev. Lett. **107**, 011802 (2011), 1104.3922.
[67] S. Parke and M. Ross-Lonergan (2016), private communication.
[68] J. M. Conrad, C. M. Ignarra, G. Karagiorgi, M. H. Shaevitz, and J. Spitz, Adv. High Energy Phys. **2013**, 163897 (2013), 1207.4765.
[69] M. Honda, T. Kajita, K. Kasahara, and S. Midorikawa, Phys. Rev. D **70**, 043008 (2004).
[70] http://icecube.wisc.edu/science/data/IC86-sterile-neutrino.
[71] B. J. P. Jones, Ph.D. thesis, MIT (2015), URL http://lss.fnal.gov/archive/thesis/2000/fermilab-thesis-2015-17.pdf.
[72] C. A. Arguelles Delgado, Ph.D. thesis, University of Wisconsin - Madison (2015), URL http://search.proquest.com/docview/1720322773.